The 2018 Structures Congress (Structures18)
Songdo Convensia, Incheon, Korea, August 27 - 31, 2018

Field application examples of an eddy current based post-tension tendon force monitoring technique

Oh-Jun KWON[1)], Jun LEE[2)] and *Hoon SOHN[3)]

[1), 2,) 3)] *Department of Civil and Environmental Engineering, KAIST, Daejeon 34141, Korea*
[1)] *koj9464@kaist.ac.kr*

ABSTRACT

Post-tensioning (PT) tendons are commonly used for assembling modularized pre-cast concrete members. The tension force in PT tendons decreases over time, and tension force reduction can eventually cause failure of entire structural systems. To address this issue, the authors group previously developed a PT tendon force monitoring system based on pulsed-eddy-current (PEC) measurements. This system estimates the tension force in PT tendons using the proportional relationship between the standard deviation of the measured PEC response and the tension force. In this study, the previously developed tendon force monitoring system is applied to tension force monitoring of two real bridges. An eddy current sensors (ECS) were installed on the anchor head surface of 50 m long tendon and on duct sheath of 100 m tendon. At each ECS, the PEC responses were measured and the tension force variation was successfully detected.

1. INTRODUCTION

Precast and pre-stressed concrete have been widely used because it has the advantages of shortening construction time and improving its durability. Especially, post-tensioning (PT) tendon is mostly used for assembling modularized pre-cast concrete members, such as long-span bridge, industrial factory building and nuclear generating station. The tension force in PT tendons decreases over time due to immediate loss and time dependent loss (Tadros et al. 2003). Excessive tension force reduction damages the integrity of the structure and may result in failure of entire structural systems. To address this issue, several techniques have been proposed to detect the tension force reduction in the PT tendons. For example, smart tendon by inserting fiber bragg grating (FBG) optical fiber into a central wire of tendon measures the strain change due to tension force variation (Kim et al 2012). However, because it

[1)] Graduate Student
[2)] Graduate Student
[3)] Professor

is necessary to make a hole in the central wire of the tendon to insert the optical fiber into the hole, the smart tendon fabrication is relatively expensive and difficult. An electromagnetic (EM) sensor detects the tension force reduction based on the Villari effect (inverse magneto-mechanical effect) of steel. (Wang et al. 2005). However, because it need to wrap sensor around the PT tendon, its applicability for a PT tendon embedded inside concrete is limited.

The authors group previously developed pulsed-eddy-current based tension-reduction-detection (PTRD) system (Kim et al. 2018). The developed PTRD system detects tension force reduction using the proportional relationship between the standard deviation of the measured PEC response and the tension force. The performance of the PTRD system was validated in the laboratory. In this paper, the developed PTRD system is applied to tension force monitoring of two real bridges. To measure the PEC responses, a compact ECS is installed on the anchor head surface of 50 m long tendon and on duct sheath of 100 m tendon. As a result of measurement, the variation of the tendon force is detected using the measured PEC responses.

This paper is organized as follows: Section 2 describes working principle overview and the hardware of the developed PTRD system. An eddy current sensor fabrication, installation and measurement result are discussed in Section 3. Section 4 concludes with a summary and future work.

2. Development of PEC-based tension-reduction-detection (PTRD) system

2.1 Overview of developed PTRD system working principle

The PTRD system was developed based on the assumption that the tension force variation in the PT tendons causes a stress change on an anchor head and consequently the variation of the PEC response. This assumption was validated using the finite element analysis program ABAQUS Standard 6.13.(Kim et al. 2018). The developed PTRD system employs the ECS and measures the PEC response to estimate stress change on the anchor head and the tension force variation.

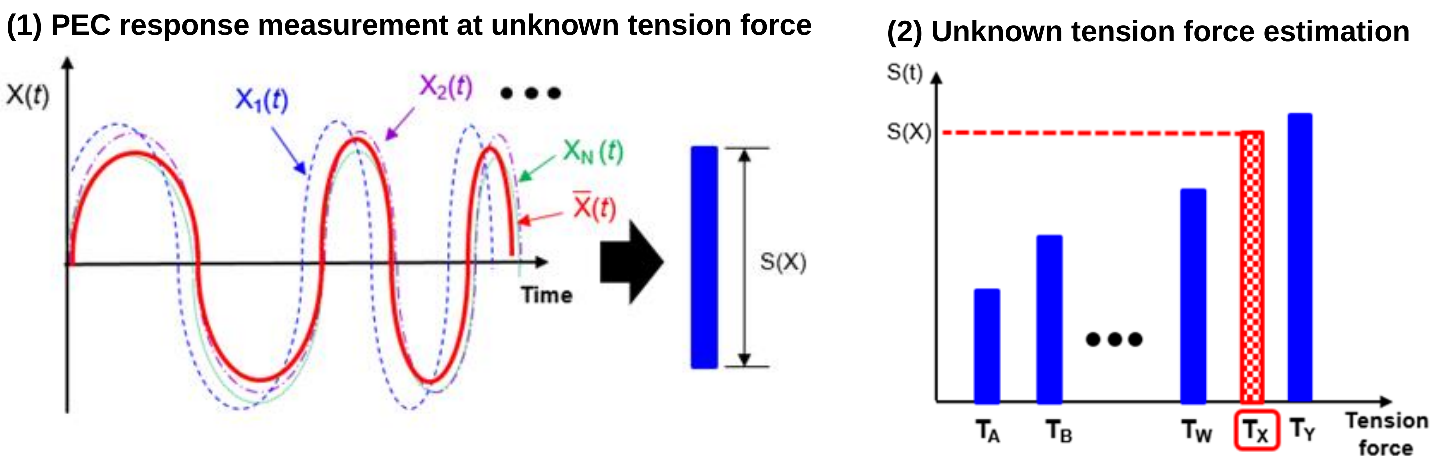

(a) (b)

Fig.1 (a) Standard deviation calculation of the PEC response; (b) estimation of the tension force

Fig. 1 provides an overview of the tension force estimation, which consists of two steps: (1) the PEC response measurement at unknown tension force during long term monitoring, and (2) unknown tension force estimation.

(1) The PEC responses are measured $\boldsymbol{N}$ times and the standard deviation S(X) is calculated (Fig. 1(a)). The standard deviation S(X) is computed using the following Eq. (1).

$$\boldsymbol{S}(\boldsymbol{X}) = \left[\sum_{i=1}^{N}\sum_{j=1}^{M}(\boldsymbol{X_i}(\boldsymbol{j}\cdot\Delta\boldsymbol{t}) - \bar{\boldsymbol{X}}(\boldsymbol{j}\cdot\Delta\boldsymbol{t}))^2/\boldsymbol{M}\cdot\boldsymbol{N}\right]^{1/2} \tag{1}$$

Where X_i(t) (i = 1, 2, …, $\boldsymbol{N}$) is the PEC responses measured at unknown tension force during long term monitoring. $\bar{X}$(t) (=$\sum_{i=1}^{N} X_i\,(t)/N$) the averaged PEC response, $\Delta\boldsymbol{t}$ denotes the sampling interval of each PEC response, and $\boldsymbol{M}$ denotes the number of sample points in each PEC response.

(2) Unknown tension force is estimated using the proportional relationship between the calculated standard deviation S(X) and the tension force (Fig. 1(b)).

2.2 Overview of developed PTRD system hardware

The developed PTRD hardware is composed of an arbitrary waveform generator (AWG), a control unit and a digitizer. The working principle of the hardware system is shown in Fig.2. First, a trigger signal is transferred to the AWG from the control unit and then the control unit synchronize the AWG and the digitizer. The AWG generates a pulsed signal and transmits pulsed signal to a driving coil of the ECS, and produced voltage in a pick-up coil of the ECS is transfer to the digitizer. The transferred analog signal is converted to a digital signal by the digitizer. The digital signal is stored in the control unit.

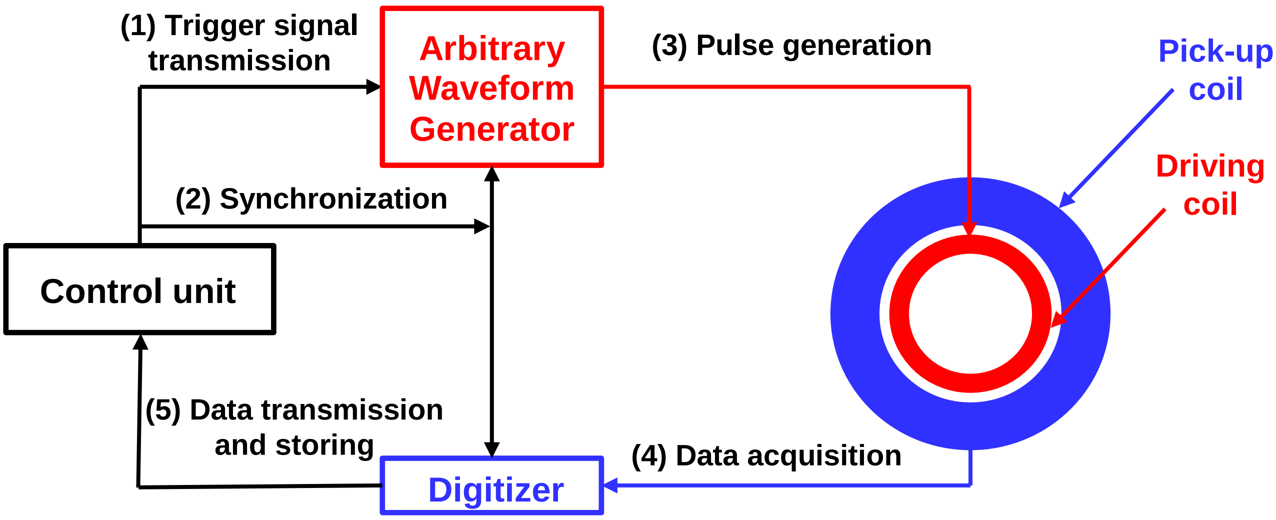

Fig. 2 Overview of the developed PTRD hardware system: a control unit, an AWG, an ECS and a digitizer

3. Field application examples

The developed PTRD system was applied to the Seoho Bridge and the Jeongleungcheon Bridge in South Korea.

3.1 Field application of the Seoho Bridge

The Seoho Bridge is located near Mapo-gu and Yongsan-gu in Seoul, South Korea and is approximately aligned in the south and north direction. This bridge is PSC box girder and RC rahmen bridge and has approximately 4,850 m total long and 18.4 ~ 25.9 m wide. As a result of the safety inspection in the Seoul city, the PT tendon failure was discovered. To complement the PT tendon, the PT tendons of 124 bon were newly installed and the PT tendons of 4 bon were replaced.

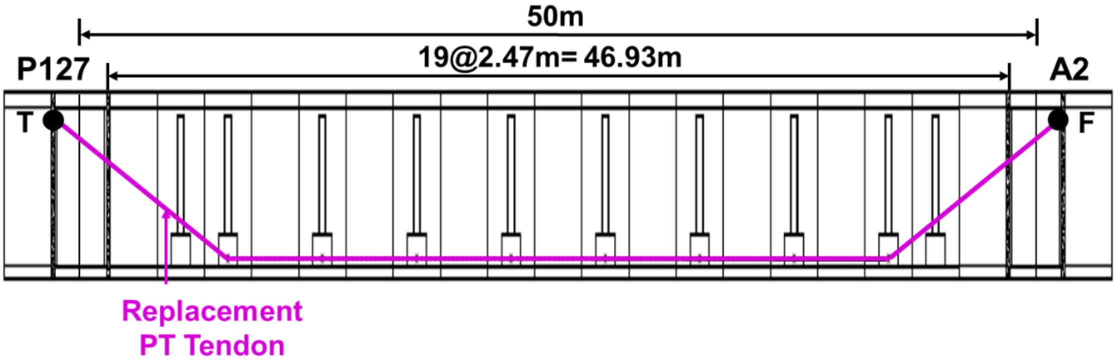

Fig. 3 A side cross-section view of the Seoho Bridge P127 – A2 girder

Fig. 3 depicts a side cross-section of the Seoho Bridge P127 – A2 girder. This girder has nineteen segments and each segment is 2.47 m long. A tensile anchorage (T) and fixed anchorage (F) were installed in P127 section and A2 section, respectively. The one-side tension was performed on the tensile anchorage using steel wire drawing jack (Fig. 4(a)) and the ECSs were installed on the anchor head surface of the fixed anchorage (Fig. 4(b)).

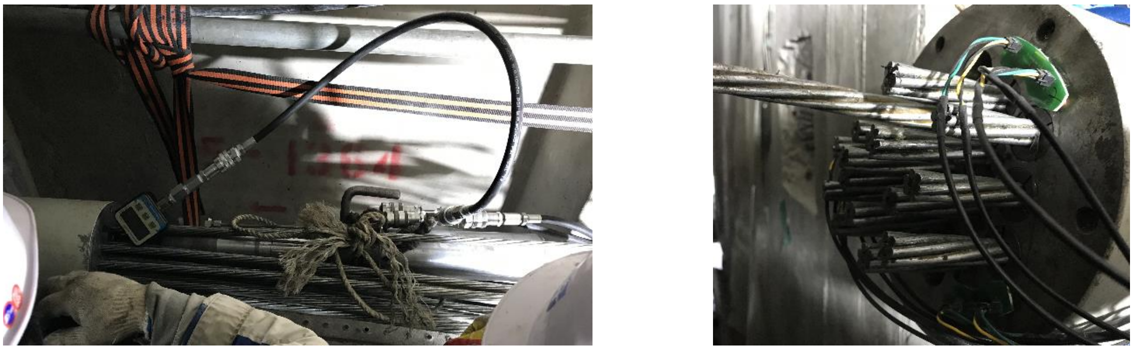

(a) (b)

Fig. 4 (a) One side tension using steel wire drawing jack; (b) ECS installation on the anchor head surface of fixed anchorage

Fig. 5(a) depicts a front cross-section of the Seoho Bridge A2 girder. In the S and N section, seventeen PT tendons were replaced and seven ECSs were installed on the anchor head surface, respectively (Fig. 5(b) and (c)). The ECS installed in Seoho Bridge is designed with the drive coil and the pick-up coil. The driving coil is placed inside of the pick-up coil to widen the sensing area for the secondary magnetic field and to increase the sensitivity to tension variation. The installed ECS properties are listed in Table 1.

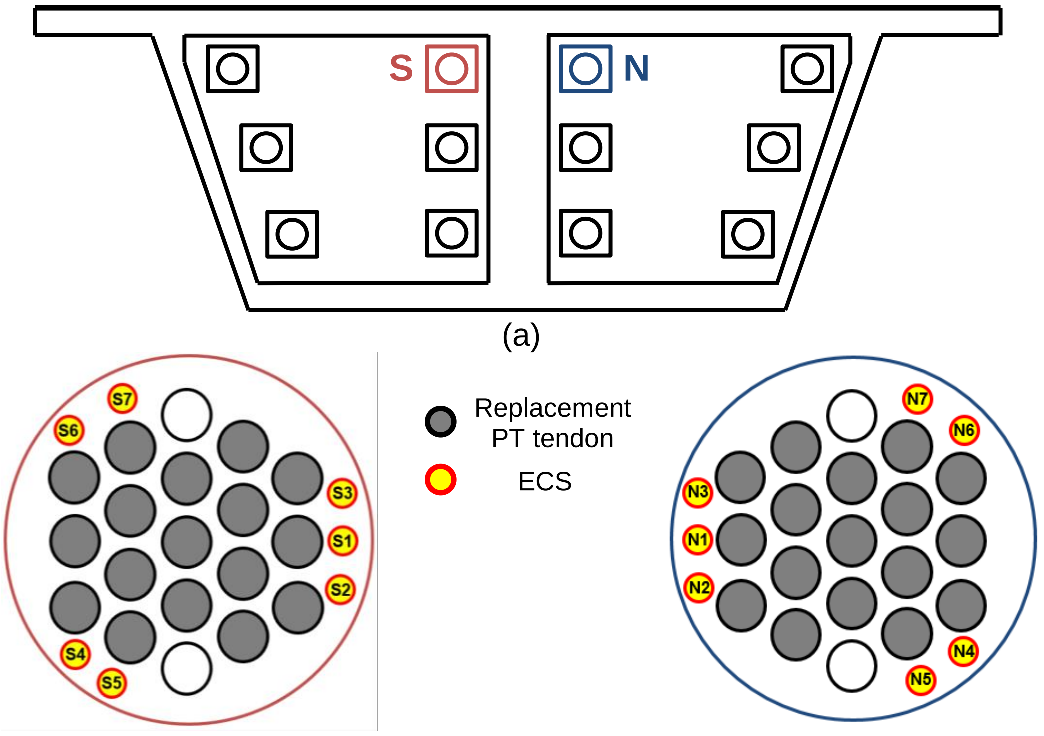

Fig. 5 (a) A front cross-section view of the Seoho Bridge A2 girder;
(b) cross-section of anchor head in S; (c) cross-section of anchor head in N

	Drive coil	Pick-up coil
Diameter	3 mm	7 mm
Number of Turns	60 turns	300 turns
Wire Diameter	0.1 mm	0.1 mm
Inductance	11.52 μH	400.8 μH
Resistance	1.49 Ω	11.2 Ω

Table 1 Properties of ECS

After the ECSs were installed, a cap was installed on the anchor head of the fixed anchorage (Fig. 6(a)) and the PEC response long-term measurement was started. The performance of the developed PTRD system was tested with the experimental setup described in Fig. 6(b). Using the SMA connector, each driving coil and pick-up coil was connected to the AWG and digitizer of the developed PTRD system. The driving coil of the ECS was excited by a 1.5 V pulsed signal with 100 μs duration. The sensing frequency was 50 MHz and the sensing time was 0.0003 s.

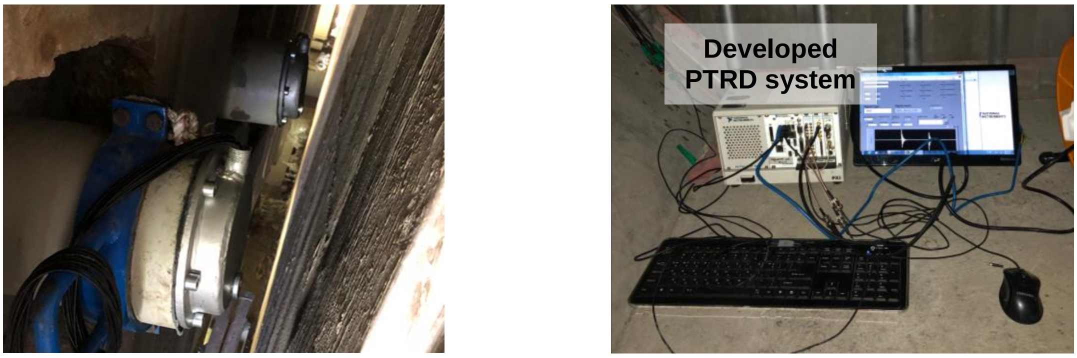

(a) (b)

Fig. 6 (a) Cap installed on the surface of anchor head; (b) experimental setup to validate the performance of the developed PTRD system

Fig. 7 shows the standard deviation of the measured PEC response for each ECS. The first, second and third test were performed on April 30, May 27 and June 27, 2018, respectively. The S2 and S7 sensors were damaged due to uncertain cause. During cap installation, the N1 ~ 7 sensors were broken as the positon change of ECSs installed on the anchor head. #1 and #2 ~ 5 are the S1 and the S2 ~ 6, respectively.

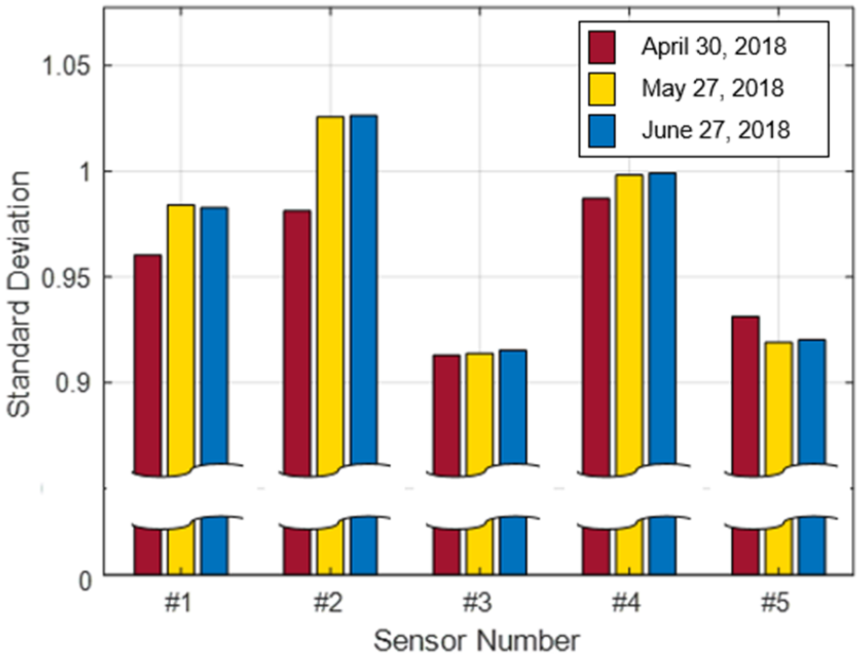

Fig. 7 Standard deviation of the measured PEC responses

Because the standard deviation difference between the first and second test occurred due to the physical property change by epoxy injection into the cap as well as the tension force variation, the variation estimation of the tension force between the first and second test is impossible. As a result of the standard deviation comparison between the second and third test, it is estimated that the tension force of the PT tendon measured by the #1 is decreased and the tension force of the PT tendons measured by the other ECSs is increased.

3.2 Field application of the Jeongleungcheon Bridge

The Jeongleungcheon Bridge is located near Seongdong-gu and Seongbook-gu in Seoul, South Korea and is approximately aligned in the west and east direction. This bridge is PSC box girder and RC rahmen bridge and is approximately 9,889 m total long and 7.5 ~ 33.7 m wide. As a result of the safety inspection in the Soul city, fracture of PT tendon 1 bon was discovered. To complement the PT tendon, the PT tendons of 25 bon were replaced.

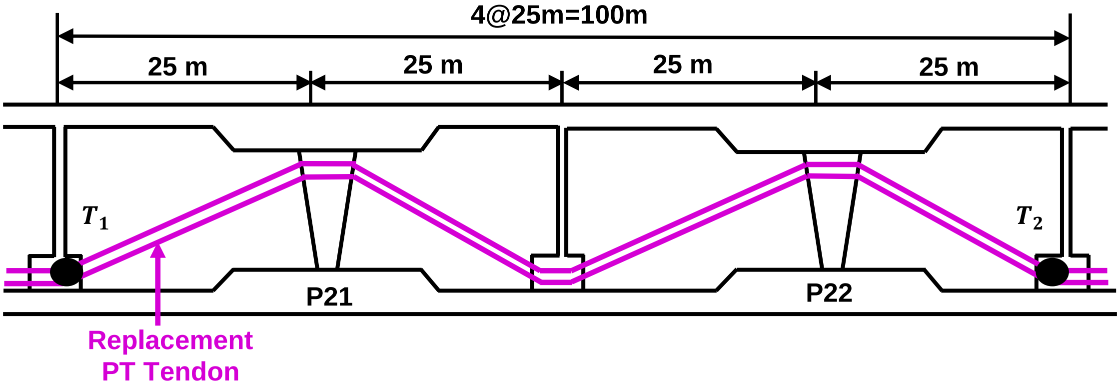

Fig. 8 A side cross-section view of the Jeongleungcheon Bridge P21-P22 girder

Fig.8 depicts a side cross-section of the Jeongleungcheon Bridge P21 - P22 girder. This girder has four segments and each segment is 25 m long. The tensile anchorages were installed in P21 section (T_1) and P22 section (T_2). The two-side tension was performed on both tensile anchorages by using steel wire drawing jack (Fig. 9(a)) and ECSs were installed on duct sheath of 100 m tendon (Fig. 9(b)).

(a) (b)

Fig.9 (a) Two side tension using steel wire drawing jack; (b) ECS installation on the duct sheath and the PT tendon between the ducts

Fig.10(a) depicts a front cross-section of the Jeongleungcheon Bridge P21 girder. In the E and W section, five type 1 and type 2 ECSs were installed on the duct sheath, respectively (Fig. 10(b) and (c)). Five type 3 ECSs were installed on the PT tendon between duct sheaths of W section (Fig. 10(c)). The ECSs of three types installed in Jeongleungcheon Bridge is designed with the drive coil and the pick-up coil. The driving coil is placed inside of the pick-up coil to widen the sensing area for the secondary magnetic field and increase the sensitivity to tension variation. The ECS properties of three types are listed in Table 2.

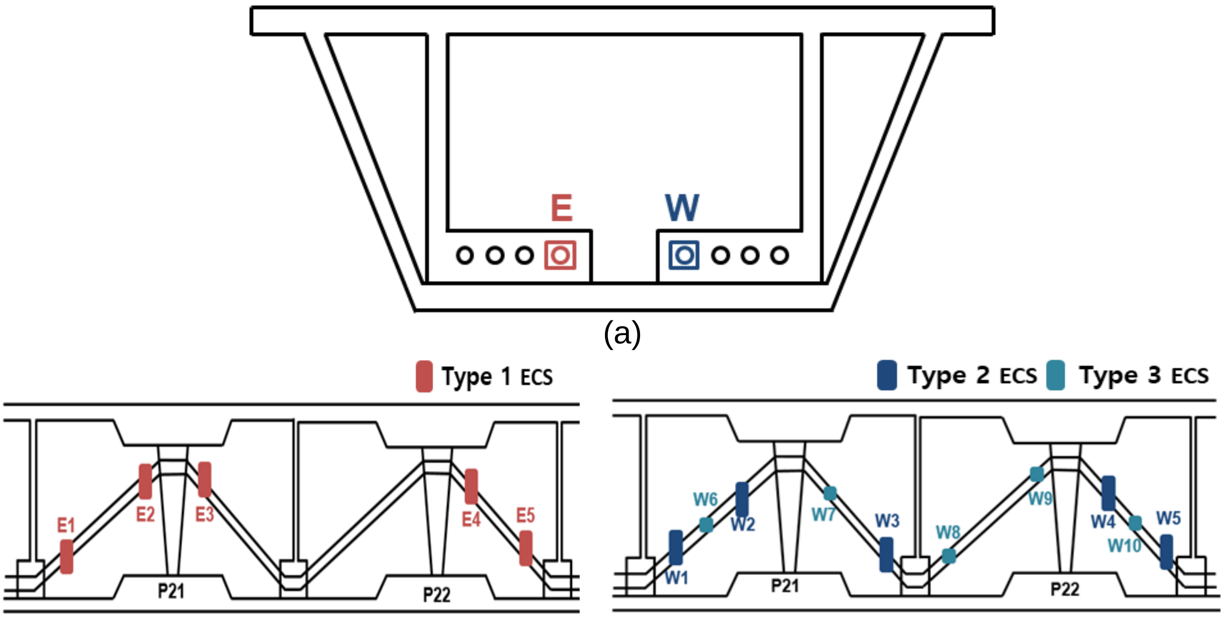

(b) (c)

Fig.10 (a) A front cross-section view of the Jeongleungcheon Bridge P21 girder; (b) side cross-section of E section; (c) side cross-section of W section

Table 2 ECS properties of three types

	Type 1	Type 2	Type 3
Diameter (Driving/Sensing)	130/154 mm	111/130 mm	99/120 mm
Number of Turns (Driving/Sensing)	72/264 turns	48/257 turns	51/276 turns
Wire Diameter (Driving/Sensing)	0.4 mm	0.4 mm	0.4 mm
Inductance (Driving/Sensing)	570 μH/400.8 mH	570 μH/400.8 mH	570 μH/400.8 mH
Resistance (Driving/Sensing)	2.8/14.4 Ω	2.8/14.4 Ω	2.8/14.4 Ω

After the ECSs were installed (Fig. 11(a)), the PT tendons were replaced and the PEC response long-term measurement was started. The performance of the developed PTRD system was tested with the experimental setup described in Fig. 11(b). Using the SMA connector, each driving coil and pick-up coil is connected to the AWG and digitizer of the developed PTRD system. The driving coil of the ECS was excited by a 1 V pulsed signal with 100 μs duration. The sensing frequency was 50 MHz and the sensing time was 0.0003 s.

(a)

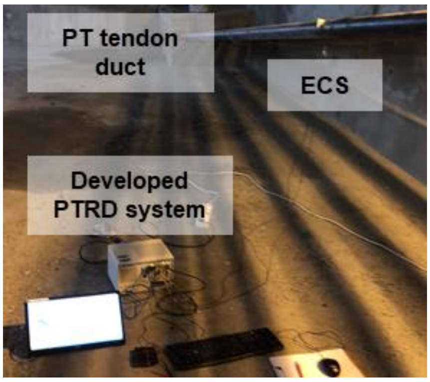

(b)

Fig.11 (a) ECS installed on the duct sheath and the PT tendon; (b) experimental setup to validate the performance of the developed PTRD system

Fig. 12 shows the standard deviation of the produced PEC response for each ECS. The first and second test were performed on May 28 and June 28, 2018, respectively. During PT tendon insertion, the W6, W7 and W9 sensors were damaged due to the friction between the PT tendon and the ECSs. #1 ~ 5, #6 ~ 10, #11 and 12 are the W1 ~ 5, the E1 ~ 5, the W8 and W10, respectively.

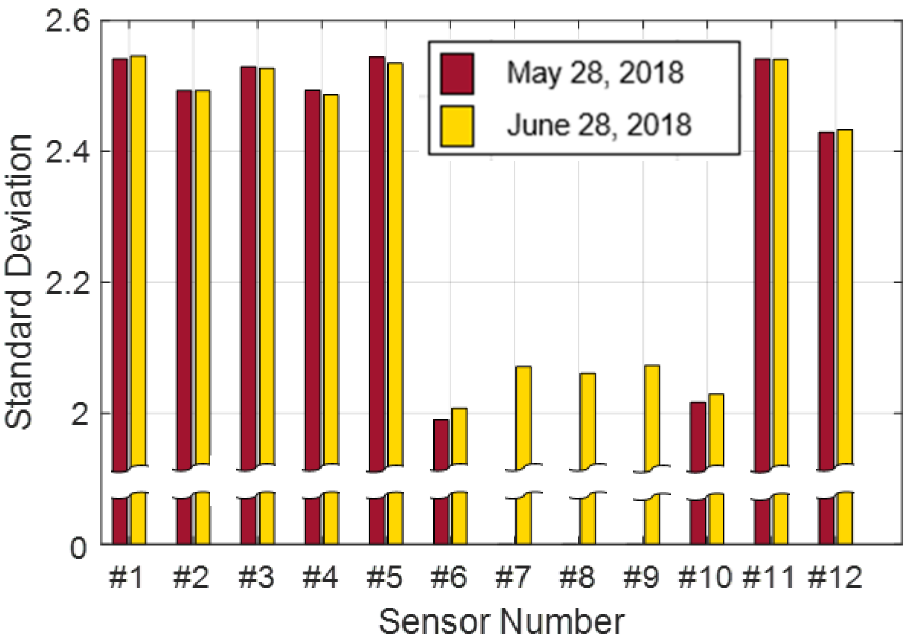

Fig. 12 Standard deviation of the measured PEC responses

As a result of the standard deviation comparison between the first and second tests, it is estimated that the tension force of the PT tendon measured by the #1, 6, 10 and 12 is increased and the tension force of the PT tendons measured by the #2, 3, 4, 5 and 11 ECSs is decreased. Because the #7 ~ 9 installed on the upper duct were not measured due to the upper duct finishing work in the first test, the variation estimation of the tension force of the PT tendon measured by the #7 ~ 9 is impossible.

4. CONCLUSIONS

In this paper, the developed PTRD system is applied to the Seoho Bridge and Jeongleungcheon Bridge for monitoring the tension force variation in the PT tendons. The applied PTRD system uses the ECS installed on the anchor head and tendon sheath and detects the tension force variation by measuring PEC responses.

During approximately two months, the PEC responses were measured three times at Seoho Bridge and two times at Jeongleungcheon Bridge. As a result of PEC responses measurement, the tension force variation in PT tensions was successfully detected. To validate the performance of field application of the PTRD system, the authors group will measure the PEC response for three years on a regular basis.

This paper has not considered the effects of environmental influence (e.g., temperature, humidity and corrosion on the anchor head) in the field. Hence, it is necessary to solve the problem of environmental compensation in order to obtain more reliable tension force detection.

REFERENCES

Tadros, M.K., Al-Omaishi, N., Seguirant, S.J. and Gallt, J.G. (2003), Prestress Losses in Pretensioned High-Strength Concrete Bridge Girders, Report No. HCHRP 496, Transportation Research Board

Wang, G., Wang, M.L., Zhao, Y., Chen, Y. and Sun, B. (2005), "Application of EM stress sensors in large steel cables", Smart Struct. Mater., 5765, 395-406.

Kim, J.M., Kim, H.W., Park, Y.H., Yang, I.H. and Kim, Y.S. (2012), "FBG sensors encapsulated into 7-wire steel strand for tension monitoring of a prestressing tendon", Adv. Struct. Eng., 15, 907-917.

Brown Jr, W.F. (1965), "Theory of magnetoelastic effects in ferromagnetism", J. Appl. Phys., 36(3), 994-1000.

Zhao X, Lord DG. Application of the Villari effect to electric power harvesting. J Appl Phys 2006;99:2014–7. http://dx.doi.org/10.1063/1.2165133.

Kim, J.M, Lee, J and Sohn, H. (2018), "Detection of tension force reduction in a post-tensioning tendon using pulsed-eddy-current measurement", *SEM,* **65**(2), 129-139.

Jiles, D.C and Atherton, D. L. (1986), "Theory of ferromagnetic hysteresis", *J. Magn. Magn. Mater.,* **61**(1-2), 48-60.

Zhao, X. and Lord, D.G. (2006), "Application of the villari effect to electric power harvesting", *J. Appl. Phys.,* **99**, 2014-2017.

Wang, G., Wang, M.L., Zhao, Y., Chen, Y. and Sun, B. (2005), "Application of EM stress sensors in large steel cables", Smart Struct. Mater., 5765, 395-406.

Kim, J.M., Kim, H.W., Park, Y.H., Yang, I.H. and Kim, Y.S. (2012), "FBG sensors encapsulated into 7-wire steel strand for tension monitoring of a prestressing tendon", Adv. Struct. Eng., 15, 907-917.